Chapter V

Anticancer Property of Complexes of Iron-Oxide Nanoparticle with Berberine and Sanazole: an *In Vitro* Study

Chapter V: Anticancer Property of Complexes of Iron-Oxide Nanoparticle with Berberine and Sanazole: an *In Vitro* Study*

Table of Contents

*****Most of the results in this chapter merited publication in the Journal of Environmental Pathology Toxicology and Oncology as- *Sreeja S, Nair CKK. Anticancer Property of Iron Oxide Nanoparticle-Drug Complexes: An in vitro Study. J Environ Pathol Toxicol Oncol. 2015; 34(3):183-9. PubMed PMID: 26349601.*

Tumor-specific targeting of chemotherapeutic molecules can increase the therapeutic efficacy of most anticancer drugs. We complexed a hypoxic cell-targeting agent sanazole (SAN) and a cytotoxic isoquinoline alkaloid berberine (BBN) on to surface-modified iron oxide nanoparticles (NPs). These nano-drug complexes were characterized by FTIR, XRD, TEM and nanosize analyser. The major objective of this study was to elucidate the molecular mechanism of cytotoxicity in murine tumor cells (DLA) induced by NP-BBN-SAN complexes. The cytotoxicity of these complexes was determined using the trypan blue dye exclusion method. The induction of apoptosis and cellular DNA damage in these cells was analyzed using dual staining and comet assay, respectively. The expression of genes in the treated cells elucidated the molecular mechanism underlying cytotoxicity. The cells treated with NP-BBN-SAN complexes showed significant increases in cytotoxicity and apoptosis, as well as extensive damage to cellular DNA compared to control cells. The cells treated with NP-BBN-SAN complexes showed greater DNA damage compared with the other treatments. The increase in the expression of a pro-apoptotic gene suggested that apoptosis was the mechanism underlying cytotoxicity induced by NP-BBN-SAN complexes. Complexing with SAN increased the cytotoxic potential of NP-BBN complexes. Further, *in vivo* studies are needed to evaluate the potential application of this method in controlling tumors.

5.1 INTRODUCTION

Berberine (BBN; 2,3-methylenedioxy-9,10-dimethoxyprotoberberine chloride) is an isoquinoline alkaloid with anticancer activity in some *in vitro* and *in vivo* systems. The anticancer potential of BBN can be extended to murine leukaemia L1210 and human uterus HeLa cell lines [Kettmann et al., 2004]. The mechanism of cytotoxicity in L1210 by BBN is the induction of apoptosis [Jantova et al., 2003]. BBN can inhibit the development of new blood vessels; therefore, it can be used to treat tumor [Tsai et al., 2004]. BBN has an anti-invasive effect on human hepatoma cells; it inhibits the expression of matrix metalloproteinase-9 and offers protection to normal liver cells [Liu et al., 2011]. BBN acted as a chemo-preventive agent against 20-methyl-cholanthrene–induced sarcoma in mice and N-nitrosodiethylamine–induced hepatocarcinogenesis in rats [Anis et al., 2001]. BBN has an inhibitory effect on human colon cancer cell proliferation and displays low toxicity in normal cells [Kotamballi et al., 2012; Murthy et al., 2012].

However, BBN showed reduced absorption by intestinal cells and resulted in gastrointestinal discomfort. The inhibitors of P-glycoprotein induced improvement in BBN absorption, revealing the role of P-glycoprotein in the intestinal absorption of BBN [Pan et al., 2002]. Nanoparticle-aided tumor targeting in cancer therapy has been found to be effective because the particles possess special properties such as small size and enhanced

permeability and retention effect. Thus, they can be easily taken up by cells and transported to the targeted tumor area.

Hypoxia is regarded as one of the major contributors to drug resistance in tumor therapy because the inner region of tumors is hypoxic, but several hypoxia sensitizers can sensitize the hypoxic tumor area. Sanazole (SAN), a nitrotriazole compound, has been shown to be efficient at sensitizing hypoxic cells, and phase III clinical trials of SAN have been completed [Karpagam et al., 2001; Martin and Nair, 2010]. Additionally, SAN has been shown to accumulate in the hypoxic milieu of tumor [Murugesan et al., 2001]. 177Lu-labeled SAN derivatives have potency in targeting tumors rather than other tissues, which indicates the efficacy of SAN in specifically targeting drugs to tumor [Das et al., 2004]. SAN significantly increases the response rate of radiotherapy and plays a significant role in local tumor control in the uterine cervix [Dobrowsky et al., 2005]. In the present study, the cytotoxic drug BBN was complexed with iron-oxide nanoparticles (NPs) and SAN to enhance the effectiveness of tumor therapy. In the present study, we investigated whether the complexing of SAN to NP–BBN complexes changed the cytotoxic potential of BBN in tumor cells *in vitro* prior to use in preclinical studies, and we further investigated the mechanism underlying this improvement.

5.2 MATERIALS AND METHODS

5.2.1 *Chemicals*

Berberine chloride was purchased from Sigma-Aldrich (St. Louis, MO, USA). All other chemicals and reagents were purchased from reputed international and national manufacturers.

5.2.2 *Preparation and characterization of Nano-drug Complexes*

Preparation and characterization of NPs were reported previously [Sreeja and Nair, 2015]. The surface-modified NPs were complexed with SAN and BBN using the sonochemical method with 0.2% solutions of each compound and characterized by FTIR, XRD, TEM and nanoanalyzer.

5.2.3 *Experiment Design*

Dalton's lymphoma ascites cells (DLA), the mouse cancer cell line, were used in this study. The cells were serially diluted and counted to 1×10^6 cells/ml for all experiments. The cells were prepared in DMEM with 12% FBS and treated as follows:

Control :cells without any treatment

NP : cells treated with NPs (200μg/ml)

BBN : cells treated with BBN (200μg/ml, 538.2nmol/ml)

SAN : cells treated with SAN (200μg/ml, 872.62nmol/ml)

NP-BBN :cells treated with NP–BBN complexes (200μg/ml NP and 538.2nmol/ml BBN)

NP-SAN : cells treated with NP–SAN complexes (200μg/ml NP and 872.62nmol/ml SAN)

NP-BBN-SAN: cells treated with NP–BBN-SAN complexes (200μg/ml NP together with 538.2nmol/ml BBN and 872.62nmol/ml SAN).

5.2.4 *Cytotoxicity Study*

The DLA cells (1×10^6cells/ml) were incubated with 200μg/ml drug and their complexes with NPs, and the cell viability was estimated using the Trypan blue dye exclusion method [Strober, 1997]. The percentage of cell death was calculated at hours 4 and 20 after incubation (detailed in chapter II). A graph of percentage mortality of cells against the treatments was plotted.

5.2.5 *Lipid peroxidation assay*

The level of lipid peroxide in the membrane was measured as malondialdehyde (MDA) in reaction with thiobarbituric acid. The level of MDA was analysed by measuring absorption at 532nm and was expressed as nanomoles per milligram of protein [Buege and Aust, 1978]. The protein levels in the sample were estimated using Lowry's method [Lowry et al., 1951].

5.2.6 *Apoptosis assay - dual staining*

Cells were washed with phosphate-buffered saline (PBS) and re-suspended in DMEM (1×10^6 cells/ml) containing 12% FBS. The induction of apoptosis was examined at hour 4 after incubation using a dual staining method with propidium iodide and acridine orange

(25µg/ml). The cells were observed under a fluorescent microscope to visualize apoptotic cells (membrane blebbing) [Duke et al., 1994] and calculated the percentage of apoptosis.

5.2.7 *Alkaline single cell gel electrophoresis*

Alkaline single-cell gel electrophoresis (comet assay) was performed on the treated cells after 4hrs of incubation. The cells were immobilized on agar matrix, lysed using alkaline lysis buffer and performed electrophoresis. After electrophoresis, the cells were visualized using propidium iodide staining (25µg/ml) and viewed under a fluorescent microscope (40X magnification) [Cerda et al., 1997; Sandeep and Nair, 2010; Nair and Nair, 2011]. Comet parameters such as tail length, % DNA in tail, tail moment, and olive tail moment were calculated using CASP [Konca et al., 2003].

5.2.8 *Studies on expression of genes involved in apoptosis*

5.2.8.1 *RNA Isolation*

RNA was isolated from the cells after 4hr incubation using acid guanidium thiocyanate-phenol-chloroform extraction method [Chomczynski et al., 1987] and quantified.

5.2.8.2 *Polymerase chain reaction*

cDNA was prepared from isolated RNA, and RT-PCR was performed for apoptotic *bax* gene, anti-apoptotic *bcl2* gene, and a housekeeping gene *β-actin* as a positive control.

5.2.9 *Statistical Analysis*

The results were presented as means ± SD and were analyzed using GraphPad PRISM software version 5. Statistical analyses of the results were performed using one-way analysis of variance (ANOVA) with the Tukey-Kramer multiple comparisons test.

5.3 RESULTS

5.3.1 *Characterization of NPs and NP-drug complexes*

The loading capacity of NPs were evaluated and the data presented in figure 5.1. The highest loading of the drugs reached when 0.2% solutions of NPs and drugs were mixed in the ratio 1 to 1.

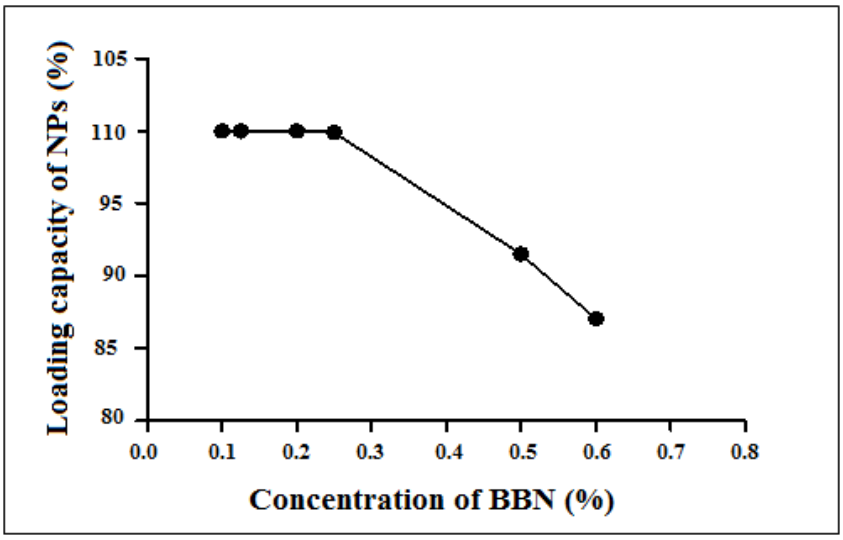

Figure 5.1: Drug (BBN) loading capacity of NPs.

We evaluated the characteristics of Fe_3O_4 nanoparticles (magnetite) prepared by co-precipitation method and its complexes with BBN and SAN by FTIR, XRD, TEM and Size analysis. As shown in the figure 5.2, the FTIR measurements was recorded in the range of 500-4000cm^{-1}. The strong peak at 3404.59cm^{-1} in NP was indicated the presence of O-H stretch in the nanoparticles. A peak observed around 2843cm^{-1} could be alloted to C-H stretching vibrations of methoxy group in BBN. The peak located around 1504.4cm^{-1} was assigned to aromatic nitro group in SAN. These peaks were also observed in NP-BBN-SAN, indicated the presence of BBN and SAN in the complexes.

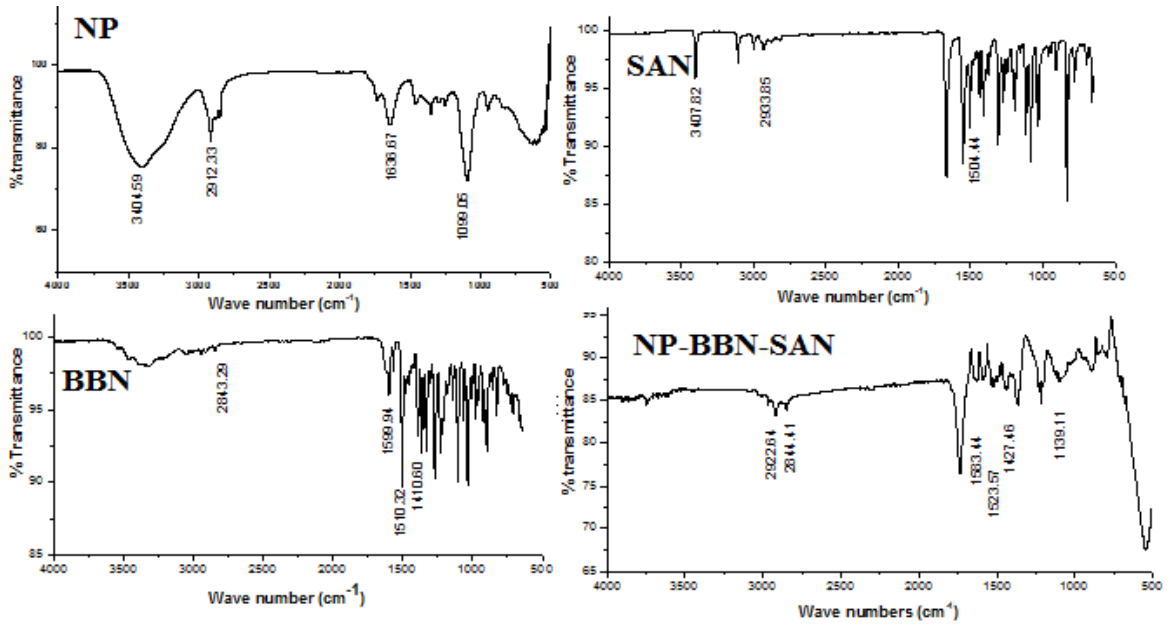

Figure 5.2: FTIR spectra of NPs, drugs and NP- drug complexes.

X- ray diffraction pattern of these nanoparticles were analysed and presented in figure 5.3. The analysis on XRD showed that the size of the NP-BBN-SAN complexes is 13.97nm based on the respective (311) peaks.TEM and Size analysis were performed to evaluate the morphology, size and hydrodynamic size of the nanoparticles. As made known in the figure 5.4, the particles were having more or less uniform size distribution of size less than 50nm with somewhat spherical shape.

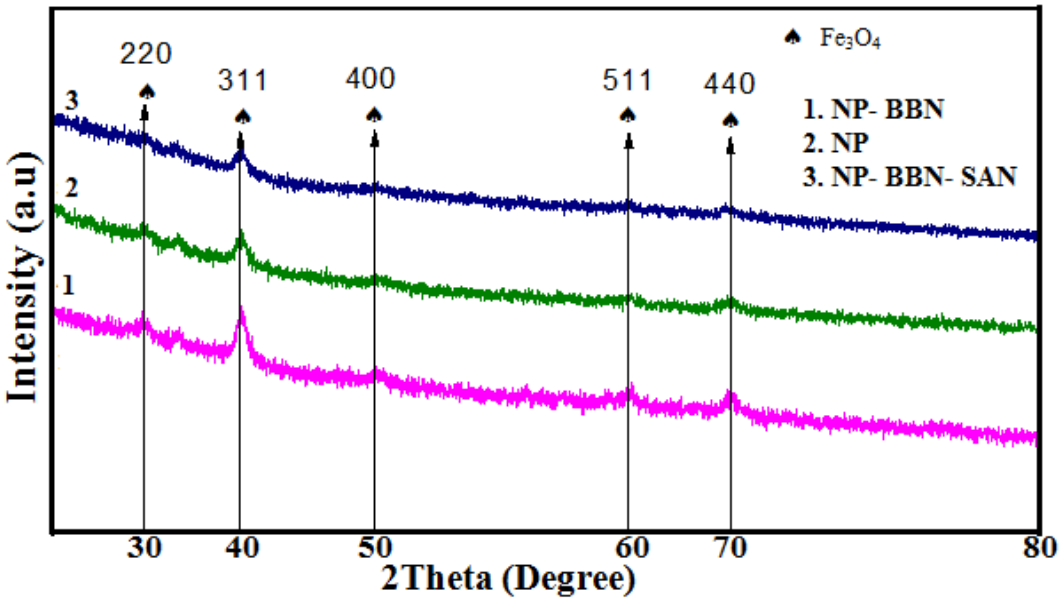

Figure 5.3: XRD pattern of NPs and its complexes with BBN and BBN-SAN.

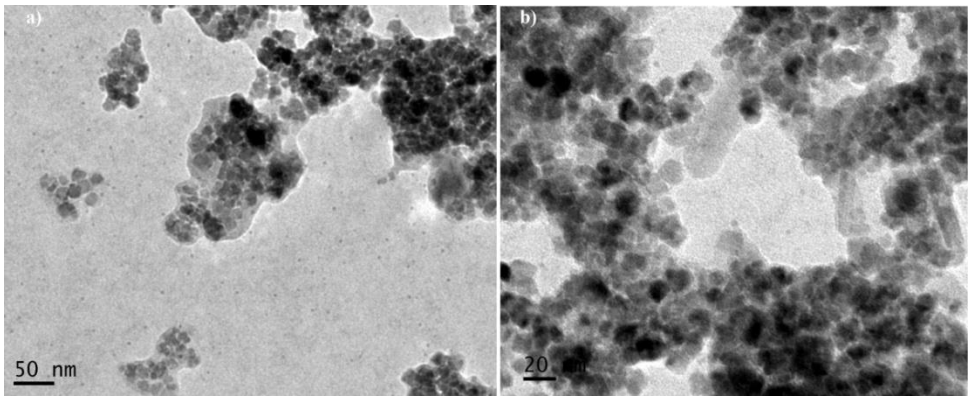

Figure 5.4: TEM images of NP-BBN-SAN complexes with scale bar a) 50nm and b) 20nm.

The size distribution pattern of NPs and NP-drug complexes were presented in figure 5.5. It can be seen that the average size of the NPs and NP-BBN-SAN complexes was 89.0 ± 59.1nm with polydispersity index (PDI) of 0.107 and 144.44 ± 94.9nm with PDI of 0.172 respectively, higher than that was obtained from TEM. Since the surface of the particles

were modified in order to increase water solubility, the particle has a tendency to bind with water molecules increases the size while dehydrated particles were usually analyzed by TEM scan.

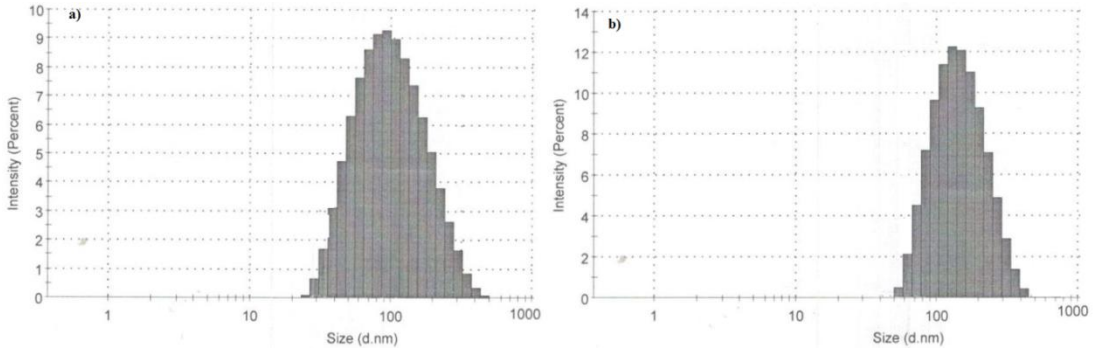

Figure 5.5: Size distribution pattern of NPs and NP-BBN-SAN complexes. Note: a) NP and b) NP-BBN-SAN complexes.

5.3.2 *Cytotoxicity Assay*

Cells were stained with Trypan blue to differentiate dead cells from live cells. Figure 5.6 represents the percentage of dead cells after 4hr and figure 5.7 presents the data of cell death at hour 20, after incubation with drugs and NP-drug complexes.

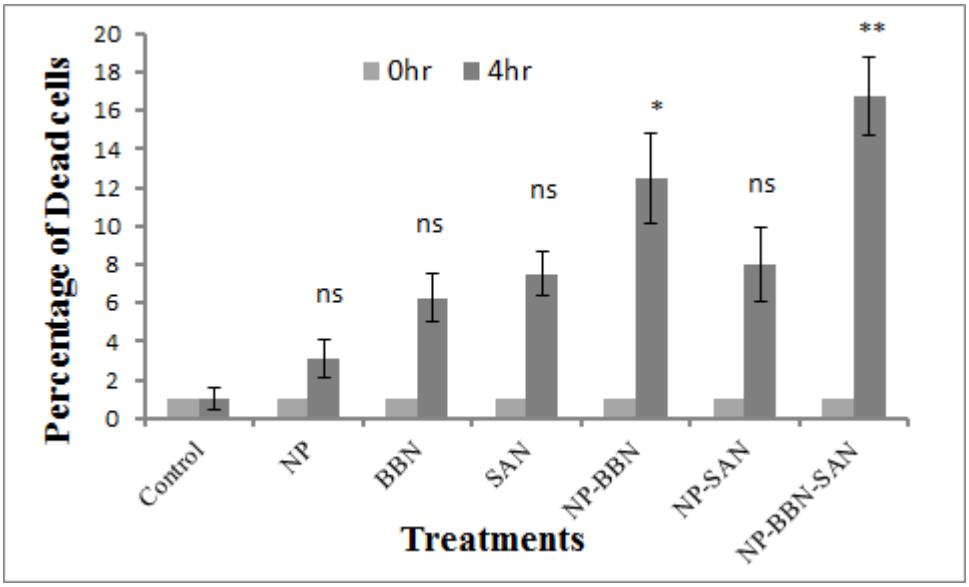

Figure 5.6: Cytotoxicity assay performed at hour 4 by Trypan blue dye exclusion method. Note: ns indicates non-significance ($P > 0.05$), * indicates significance ($P < 0.05$), and ** indicates significance ($P < 0.01$) compared with respective controls.

In the cells treated with NP-BBN-SAN complexes, 16% cell death can be seen, whereas only 6% cell death occurred in cells treated with BBN alone and 12% cell death occurred in NP-BBN-treated cells. A significant increase in the percentage of cell death in NP-BBN-SAN complexes treated cells was observed compared with the control and other treatments. The percentage of dead cells in NP-BBN-SAN treated cells increased significantly by hour 20 after incubation compared with the control and other treatments. This result indicates that there was no reduction in the cytotoxic potential of BBN after it was complexed with NPs and SAN.

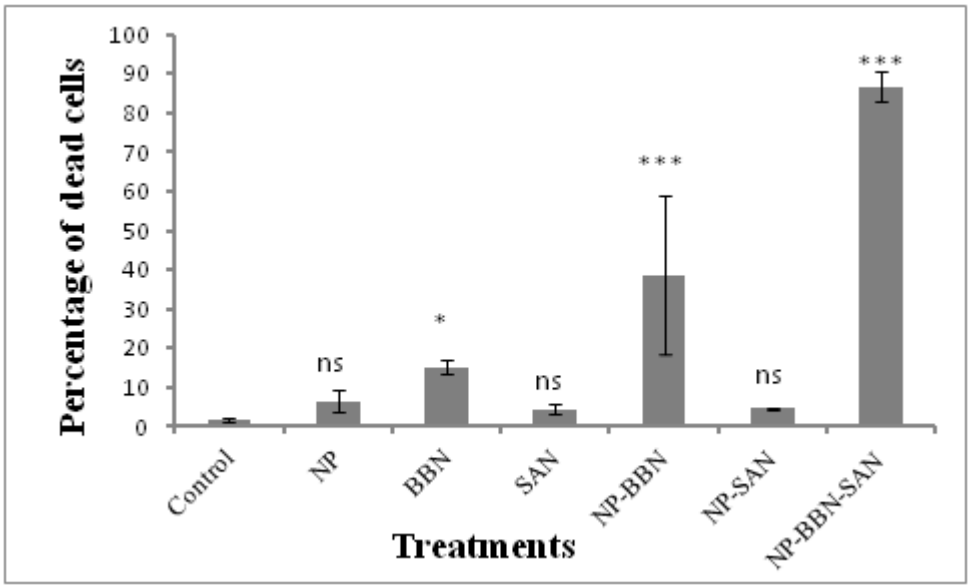

Figure 5.7: Cytotoxicity assay performed at incubation hour 20. Note: ns indicates non-significance (P>0.05), * indicates significance (P < 0.05), and *** indicates significance (P<0.001) compared with the respective controls.

5.3.3 *Induction of Apoptosis*

The apoptosis assay was performed to reveal the mechanism behind the cytotoxicity induced (Figure 5.8 and 5.9). The percentage of cells with membrane blebbing (Figure 5.8), the most common characteristic of apoptosis, was higher in cells treated with BBN alone as well as NP-BBN and NP-BBN-SAN complexes, suggesting that apoptosis was involved in cytotoxicity.

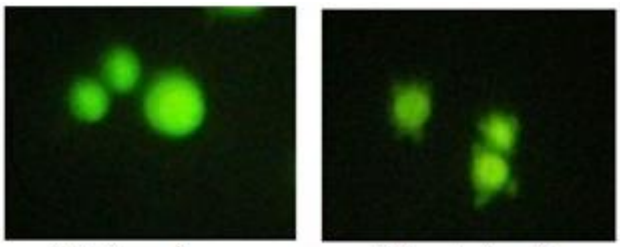

Figure 5.8: Images of normal and apoptotic cells.

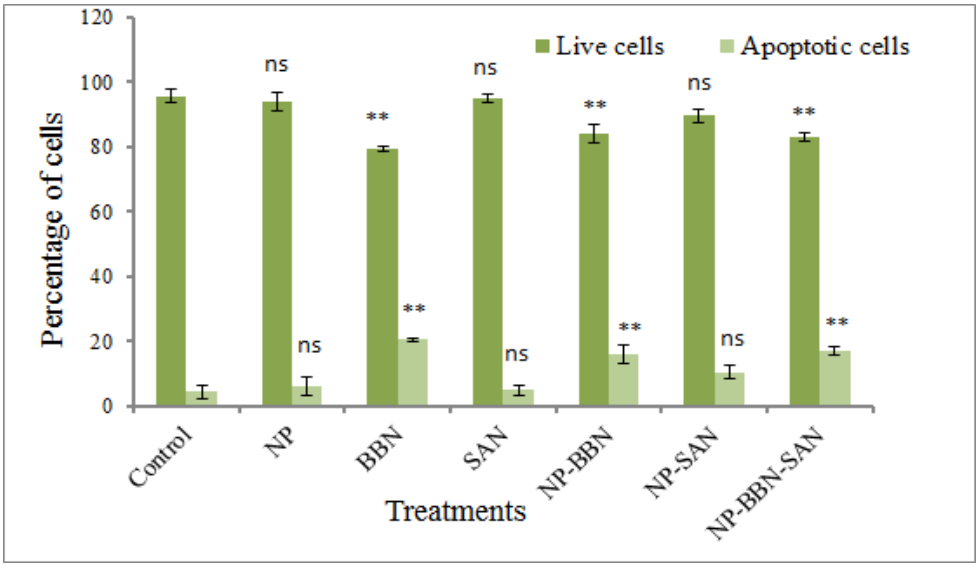

Figure 5.9: Apoptosis assay using the dual staining method. Note: ns indicated non-significance ($P>0.05$) and ** indicates significance ($P<0.01$) when compared with respective controls.

5.3.4 *Analysis of Strand Breaks in Cellular DNA*

The comet assay was performed to determine whether the treatment induced strand breaks in DNA following various treatments. The comet-shaped cells were found frequently in cells treated with NP-BBN-SAN compared with BBN alone and NP-BBN-treated cells (Figure 5.10). This result may be attributable to the synergistic action of the drugs. The comet parameters also increased significantly in the cells following treatment with NP-BBN-SAN complexes compared with the control and BBN-treated cells (Figure 5.11).

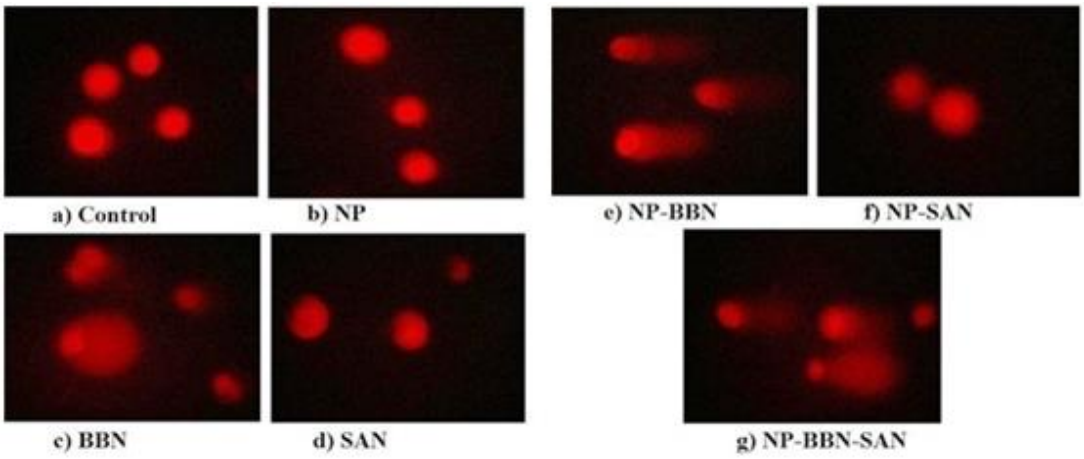

Figure 5.10: Images of cells after comet assay.

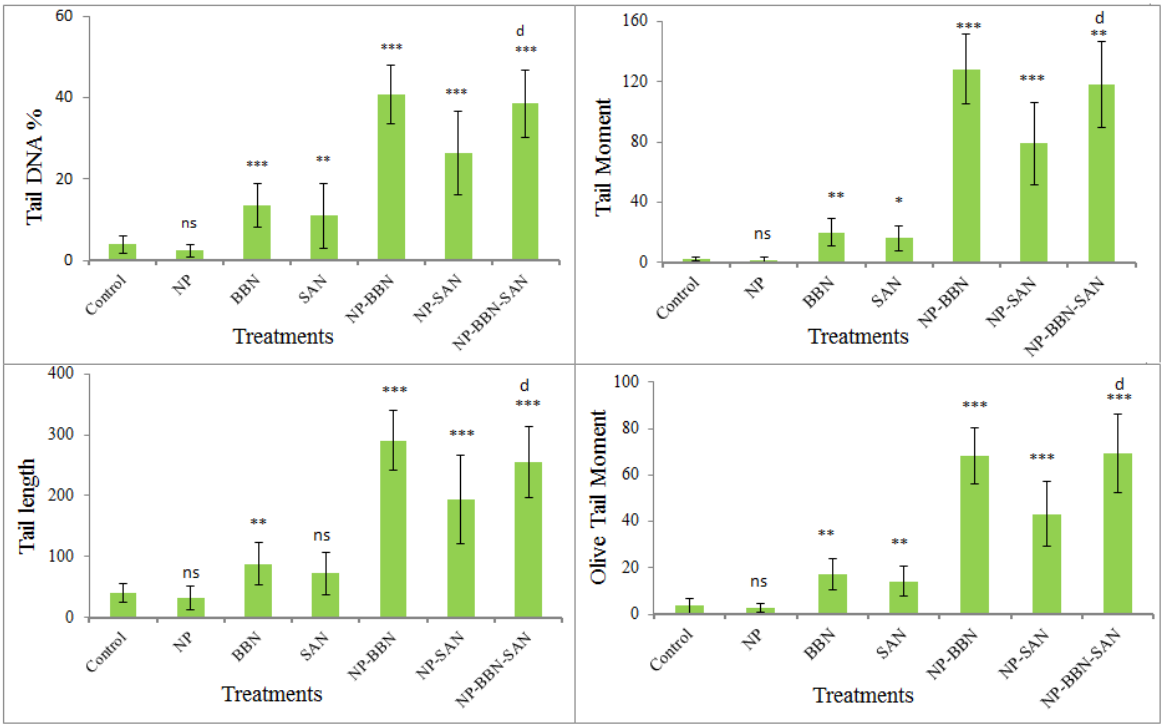

Figure 5.11: Comet parameters. Note: ns indicates non-significance (P > 0.05), * indicates significance (P < 0.05), ** indicates significance (P < 0.01), and *** indicates significance (P < 0.001) compared with respective controls. d indicates significance (P < 0.001) compared with BBN.

5.3.5 *Membrane Damage Analysis*

MDA levels were calculated as a measure of membrane damage by lipid peroxidation (Figure 5.12). The level of MDA was significantly increased in NP-BBN-SAN treated cells compared with the control and other treatments. No significant increase of MDA

levels was observed in BBN or NP-BBN treatments, suggesting the increased cytotoxic potential of NP-BBN-SAN complexes.

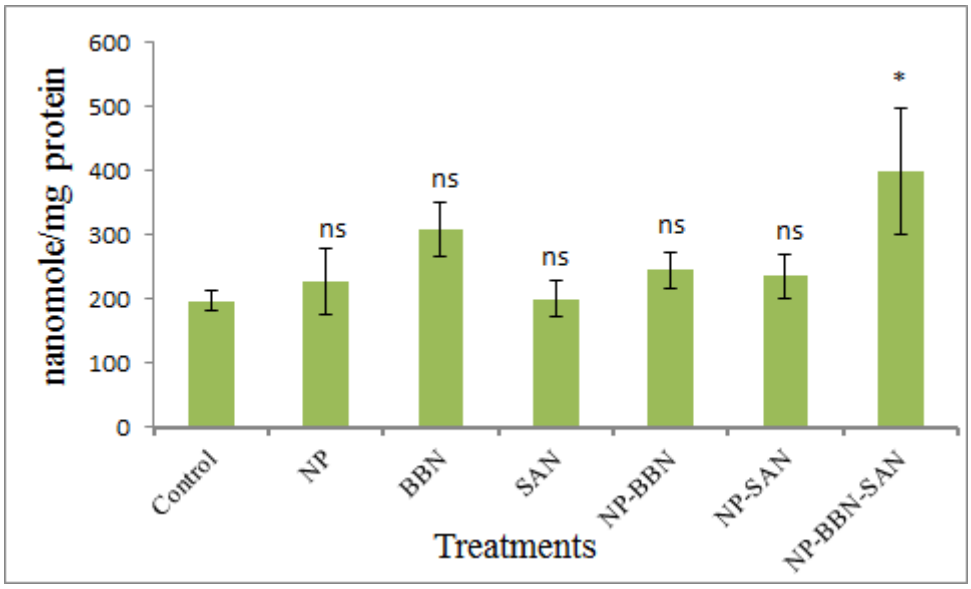

Figure 5.12: Levels of MDA in cells after various treatments. Note: ns indicates non-significance ($P>0.05$) and * indicates significance ($P<0.05$) when compared with respective controls.

5.3.6 *Study on the Expression of Genes by PCR*

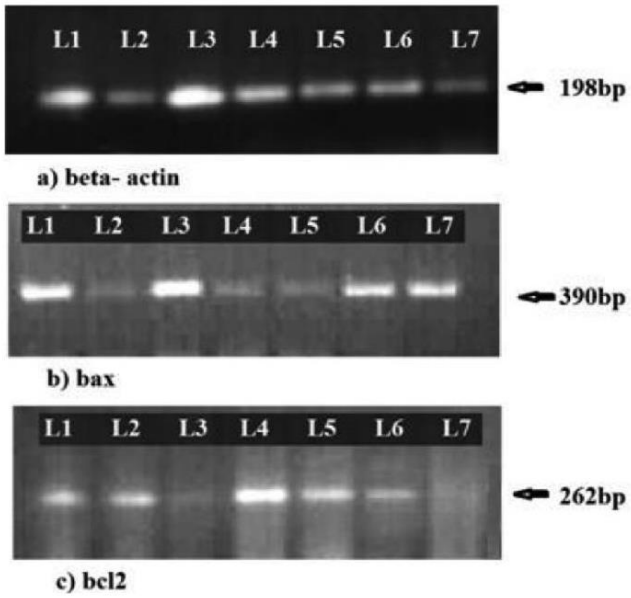

Figure 5.13: Images of gel with the expression bands of genes: *beta-actin*, *bax*, and *bcl2*. L1: Control (untreated); L2: NP; L3: BBN; L4: SAN; L5: NP-BBN; L6: NP-SAN; and L7: NP-BBN-SAN.

The higher *bax* to *bcl2* ratio is important for apoptosis.The expression of the apoptotic gene *bax*and anti-apoptotic gene *bcl2* in BBN alone as wellas NP–BBN and NP–BBN-SAN complexes arepresented in figure 5.13. In the cells treated with BBNalone as well as NP–BBN-SAN complexes, littleexpression of *bcl2* and higher expression of *bax*were observed; these results corroborate the datapresented in figures5.9.

5.4 DISCUSSION

Iron-oxide NPs have magnetic property and are of great importance because of their biocompatibility. These NPs are broken down to ferric ions and can interact with transferrin to be transported to the cytoplasm. In the cytoplasm, the protein ferritin can take up these ions, which follow normal metabolism in the body [Nakamura et al., 2000]. In an earlier report, we showed that "the chemotherapeutic effect of doxorubicin could be considerably enhanced by combination of the drug-conjugated magnetic Fe_3O_4 nanoparticles and targeted drug delivery with the application of an external magnet" [Jayakumar et al., 2009]. In the present study, the conjugation of SAN with the complexes of NP and cytotoxic alkaloid BBN (NP-BBN-SAN) was found to be more efficient in cell killing than BBN and NP-BBN alone. The mechanism underlying this cytotoxicity is the induction of apoptosis as shown by dual staining and comet assay. This mechanism was further confirmed by the expression profiling of genes involved in apoptosis. As SAN can accumulate in hypoxic tumor sites [Das et al., 2004], the NP-BBN-SAN complexeswill have greater retention at the solid tumor site and will probably affect cellular killing of tumor cells while sparing normal cells.

5.5 CONCLUSION

NP-BBN-SAN complexes induced cytotoxicity in murine tumor cells. This cytotoxicity was the result of induction of apoptosis in the tumor cells by these complexes. The results reveal the potential application of the nano-complexes in controlling tumors in vivo, as these complexes are biocompatible, and can be targeted specifically to the tumor milieu.